Site-specific incorporation of biotinylated amino acids to identify surface-exposed residues in integral membrane proteins

Justin P Gallivan[1], Henry A Lester[2] and Dennis A Dougherty[1]

Background: A key structural issue for all integral membrane proteins is the exposure of individual residues to the intracellular or extracellular media. This issue involves the basic transmembrane topology as well as more subtle variations in surface accessibility. Direct methods to evaluate the degree of exposure for residues in functional proteins expressed in living cells would be highly valuable. We sought to develop a new experimental method to determine highly surface-exposed residues, and thus transmembrane topology, of membrane proteins expressed in *Xenopus* oocytes.

Results: We have used the *in vivo* nonsense suppression technique to incorporate biotinylated unnatural amino acids into functional ion channels expressed in *Xenopus* oocytes. Binding of ^{125}I-streptavidin to biotinylated receptors was used to determine the surface exposure of individual amino acids. In particular, we studied the main immunogenic region of the nicotinic acetylcholine receptor. The biotin-containing amino acid biocytin was efficiently incorporated into five sites in the main immunogenic region and extracellular streptavidin bound to one residue in particular, α70. The position of α70 as highly exposed on the receptor surface was thus established.

Conclusions: The *in vivo* nonsense suppression technique has been extended to provide the first in a potential series of methods to identify exposed residues and to assess their relative exposure in functional proteins expressed in *Xenopus* oocytes.

Addresses: [1]Division of Chemistry and Chemical Engineering and [2]Division of Biology, California Institute of Technology, Pasadena, CA 91125, USA.

Correspondence: Dennis A Dougherty
E-mail: dad@igor.caltech.edu

Key words: biotin/streptavidin, *in vivo* suppression, surface exposure, transmembrane topology, unnatural amino acids

Received: **24 July 1997**
Accepted: **27 August 1997**

Chemistry & Biology October 1997, **4**:739–749
http://biomednet.com/elecref/1074552100400739

© Current Biology Ltd ISSN 1074-5521

Introduction

Determining the transmembrane topology of integral membrane proteins such as ion channels and neurotransmitter transporters is a necessary first step in evaluating their structure and function at the molecular level [1]. After the topology has been established, a more demanding question is the relative exposure of individual residues to the intracellular or extracellular media. Knowledge of transmembrane topology and exposure allows one to identify regions of a protein that may become glycosylated or form binding sites for external ligands, to identify intracellular regions that may be subject to phosphorylation, to assign potential binding sites for other intracellular secondary messengers (such as G proteins), and to make predictions regarding the overall structure and function of an integral membrane protein.

The present study addresses the 'higher resolution' issue of surface exposure. We wished to determine which residues are clearly on the 'outside' surface of a receptor. Of course, if a residue is determined to be exposed then the topology question is answered. Residue accessibility is clearly a related measure of protein structure, but, as discussed below, it addresses a somewhat different issue. Here, we consider a relatively well-understood membrane protein, the nicotinic acetylcholine receptor (nAChR). There is general agreement concerning the overall topology of this receptor, although final proof will require high-resolution structural data. Each subunit is thought to have a large, extracellular amino-terminal domain, followed by four transmembrane regions and a necessarily extracellular carboxyl terminus (Figure 1a). Little is known about the relative exposures of residues throughout the receptor, however.

Many other membrane channels, transporters, and receptors have less well-understood topologies. The first step (and, unfortunately, often the last step) in determining the topology is the generation of a hydropathy plot based on the protein sequence. Although hydropathy plots are useful in suggesting a possible topology for a membrane protein, they are by no means an effective substitute for experimental evidence. For instance, the primary amino-acid sequence for the ionotropic glutamate receptor was first determined in 1989 and led to a topological model analogous to that for the nicotinic receptor — four transmembrane domains and extracellularly located amino and carboxyl termini [2]. Subsequent work showed that the putative second transmembrane domain is likely to form a reentrant loop, so that the amino and carboxyl termini are on the opposite sides of the membrane (Figure 1b) [3,4].

Figure 1

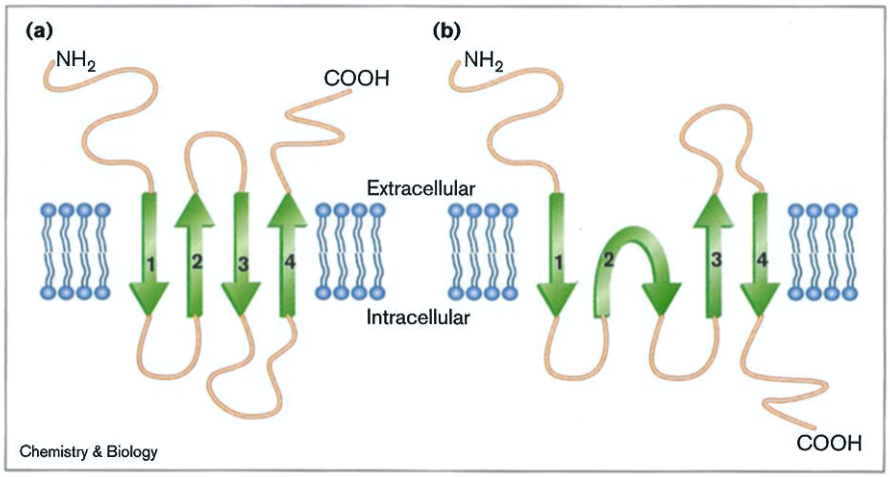

The topology of the nicotinic acetylcholine receptor (nAChR) and glutamate receptor (GluR3). **(a)** The generally accepted topology of each subunit of the nAChR. This is also the original topology model (1989–1995) proposed for GluR3 [2]. **(b)** The revised topology for the glutamate receptor [3,4].

Such a drastic change certainly alters one's view of the structure and mode of action of the receptor. Other recent experiments on a variety of ion channels and transporters, including the potassium channel ROMK1 [5], the GABA transporter GAT-1 [6], the glycine transporter GLYT1 [7], and the Na^+/glucose co-transporter SGLT1 [8], have suggested inconsistencies in the transmembrane topologies predicted from hydropathy analysis.

These studies underscore the importance of having definitive experimental approaches to determine the transmembrane topology of membrane proteins. Although several methods are available, a new approach would be welcome if it could overcome some of the inherent weaknesses of the existing methods.

Approaches for determining topology/accessibility

A wide variety of techniques have been developed to address the topology issue [1]. Below, we briefly describe some of the higher precision approaches that target specific regions of integral membrane proteins.

Endogenous glycosylation sites and N-glycosylation scanning mutagenesis

One of the most common methods for determining transmembrane topology is to assay a particular region of a protein for endogenous N-linked glycosylation. Because N-linked glycosylation occurs on the luminal side of the endoplasmic reticulum, with few exceptions [9] only regions destined to become extracellular are glycosylated. Thus, identifying a site that is glycosylated in the wild-type protein is good evidence that it is located extracellularly. Expanding upon this tactic, one can engineer N-linked glycosylation sites into transmembrane proteins to determine topology. This approach has been used recently to assay the transmembrane topologies of many ion channels and transporters, including GAT1 [6], GLYT1 [7], CFTR [10], and SGLT1 [8]. In all these studies, the functional competence of the glycosylated mutants was often quite poor compared with that of the wild-type protein and in many cases the modified proteins did not function at all. This is of particular concern because the introduction of a non-native glycosylation site may alter topology [4]. If a particular protein is found to be glycosylated in the experiment but does not function, it is often difficult to determine whether the protein fails to function because glycosylation interferes with the normal function of the protein or because glycosylation has caused the protein to fold with an altered topology.

Cysteine accessibility/substituted-cysteine accessibility

Another common method for determining transmembrane topology is the introduction of cysteine residues into the protein of interest, followed by labeling with thiol-reactive reagents. If the reagent is membrane-impermeant, topology can be evaluated by comparing the results of intracellular versus extracellular application [11,12]. For example, cysteines have been modified with biotin-containing reagents, and the reaction detected by streptavidin binding [13,14]. The cysteine modification approach has an advantage over glycosylation methods in that a single cysteine mutant is often less perturbing to the overall protein structure than the introduction of a glycosylation site. The method has been generalized by Karlin and coworkers [15,16] to the substituted-cysteine accessibility method (SCAM), allowing the 'accessibility' of specific residues to be probed with relatively small thiol-reactive reagents. Note that such accessibility is quite different from 'exposure' as used here. SCAM has labeled residues that nominally lie in a transmembrane region, but which are nonetheless accessible because they lie along an ion channel or within an agonist-binding site. Potential disadvantages of these methods arise from the contributions of endogenous cysteine residues that may also be labeled in

the assay. In addition, the introduction of new cysteines may lead to improper disulfide bond formation and incorrectly folded proteins. A possible solution to these problems is to mutate all the endogenous cysteines to another amino acid and then to introduce a unique cysteine. This has been successful in some proteins, but there are certainly cases where removal of all the endogenous cysteines will render the protein nonfunctional. Furthermore, for an *in vivo* assay, there may be complications arising from reactive cysteines found in endogenous cellular proteins that cannot be mutated away.

Epitope protection

In this type of assay, a fusion is created between the protein of interest and a well-defined epitope that is recognised by a specific antibody [4,17,18]. The fusion proteins are synthesized *in vitro* in the presence of microsomal vesicles so that the expressed protein is inserted into the membrane. Digestion of the translation mixture with proteases cleaves extramicrosomal (cytoplasmic) regions, destroying the epitope if it is displayed in this region. If the epitope is located inside the vesicle, it is protected from protease digestion and can be immunoprecipitated or detected in a western immunoblot. There are several concerns raised by this assay, however. The assay is performed in a cell-free system and the topology may not, therefore, be identical to that in an intact cell [18]. The epitope introduced is often quite large (the prolactin epitope is 195 amino acids) and consequently must often be introduced as a carboxy-terminal fusion to a truncated and often non-functional protein [4]. Finally, there is always a concern that the introduction of a large epitope may cause the protein of interest to fold improperly. This potential problem, coupled with the fact that the proteins often cannot be assayed for function, makes the assay less attractive.

Tyrosine iodination

Very recently, Hucho and coworkers [19] used ^{125}I labeling to probe surface exposure of tyrosine residues of the nicotinic receptor harvested from *Torpedo californica*. This method has some attractive features, but, because all exposed tyrosines are labeled simultaneously, one must sequence the labeled protein to determine exposure. This is not feasible with proteins for which there is not a plentiful natural source.

The biocytin approach

To address the potential shortcomings of the methods available at present, we sought to develop a new experimental approach to discover surface-exposed residues. Our design goals were as follows: to determine the surface exposure/topology of a protein *in vivo*; to assay functional proteins with wild-type behavior; to introduce a single, minimally perturbing mutation; to use a marker that is endogenous neither to the protein of interest nor to other cell-surface proteins; to detect the marker using robust and readily available methods; and to produce a graded series of reagents that allows conclusions about relative exposures. As a first step, we have combined two commonly used assay components: the biotin–streptavidin interaction and the *in vivo* nonsense suppression method.

Biotin is a small molecule that binds with high affinity ($K_d \sim 10^{-15}$ M) to streptavidin, a 60 kDa tetrameric protein. Biotin can be readily functionalized at its carboxyl terminus while retaining its ability to bind tightly to streptavidin, rendering it an ideal probe [20–22]. Biotinylated amino acids have previously been incorporated into proteins *in vitro* by supplementing the translation mixture with full-length lysyl-tRNA functionalized with biotin derivatives at the ε-amino group of lysine, thus leading to random incorporation of biotinylated amino acids at various lysine sites in the protein [23]. Although this suggested that biosynthetic incorporation of biotinylated amino acids was possible, the remaining challenge was to introduce the biotin label site-specifically in the protein of interest in a living cell. To accomplish this we employed the nonsense suppression method for incorporation of unnatural amino acids into proteins [24–27], as adapted in our laboratories for the *in vivo* heterologous expression system of the *Xenopus* oocyte [28–33].

In the *in vivo* nonsense suppression method, the oocyte is co-injected with two mutated RNA species: mRNA synthesized *in vitro* from a mutant cDNA clone containing a stop codon (TAG) at the amino acid position of interest, and a suppressor tRNA that contains the complementary anti-codon sequence (CUA) and has the desired unnatural amino acid chemically acylated to the 3′ end. During translation by the oocyte's synthetic machinery, the unnatural amino acid is specifically incorporated at the position in the protein encoded by the mRNA. Recent studies in our laboratories have shown that this method is broadly applicable, being compatible with many different proteins, a large number of sites in a given protein, and a wide range of amino acids.

As a test amino acid we chose biocytin (Figure 2), a naturally occurring (but not translationally incorporated) biotinylated amino acid. Biocytin's relatively small size, similarity to the natural amino acid lysine, and commercial availability made it particularly attractive. To test the biocytin method, we chose the prototype ligand-gated ion channel, the nAChR, a 290 kDa pentameric ion channel found at the neuromuscular junction (Figure 3) [34–38]. In particular, we chose to evaluate the main immunogenic region (MIR) of the α subunit. The MIR is composed of ten residues in the amino-terminal region of the α subunit (residues 67–76; α67–76) and binds many antibodies, including those associated with myasthenia gravis, a human autoimmune disease [39–41]. Furthermore, this region has

Figure 2

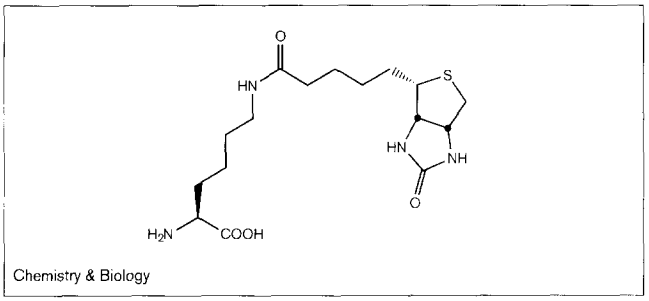

The structure of biocytin, a naturally occurring (but not translationally incorporated) amino acid.

been shown by electron microscopy to be located near the synaptic end of the nAChR [42]. Because it is known to be topologically extracellular and accessible as a unit to large proteins, the MIR appeared to be an ideal location to test the biocytin methodology for evaluating the surface exposure of individual residues. Given the tight fit between biotin and streptavidin, we anticipated that only the most highly exposed positions of the MIR would form strong biocytin/streptavidin complexes.

Results and discussion

We first mutated the codons for each of the ten residues of the MIR of the nAChR from mouse muscle (α67–76; see Table 1 for sequence) to the stop codon TAG. We then co-injected *Xenopus* oocytes with a mixture of mutant mRNA (1.2 ng total/oocyte; 4:1:1:1 α:β:γ:δ subunit stoichiometry) containing the TAG codon at a single position in the α subunit and an aminoacyl-tRNA (25 ng/oocyte) charged with the amino acid of interest. After 36–48 h, oocytes were assayed electrophysiologically for their response to 200 μM acetylcholine (ACh) by the two-electrode voltage-clamp technique [43]. The results from a successful biocytin incorporation are shown in Figure 4. In this experiment, biocytin incorporation was successful at both positions α70 and α76. Suppression with a natural amino acid (α76, tyrosine) and experiments using uncharged tRNA (tRNA–dCA) [28,29] were performed as controls. Clearly, the biotinylated mutants functioned at levels comparable to those for mutants suppressed with a natural amino acid. In addition, the very small currents arising from the dCA control (uncharged tRNA) demonstrate that the currents observed in the biocytin experiments arise solely from receptors containing the biotinylated amino acid.

At five of the ten positions in the MIR (α68, α70, α71, α75 and α76), biocytin was incorporated efficiently into functional receptors with whole-cell currents ranging from several hundred to several thousand nA (Table 1). At the other five positions (α67, α69, α72, α73 and α74) whole-cell currents were generally < 200 nA. In each experiment,

Figure 3

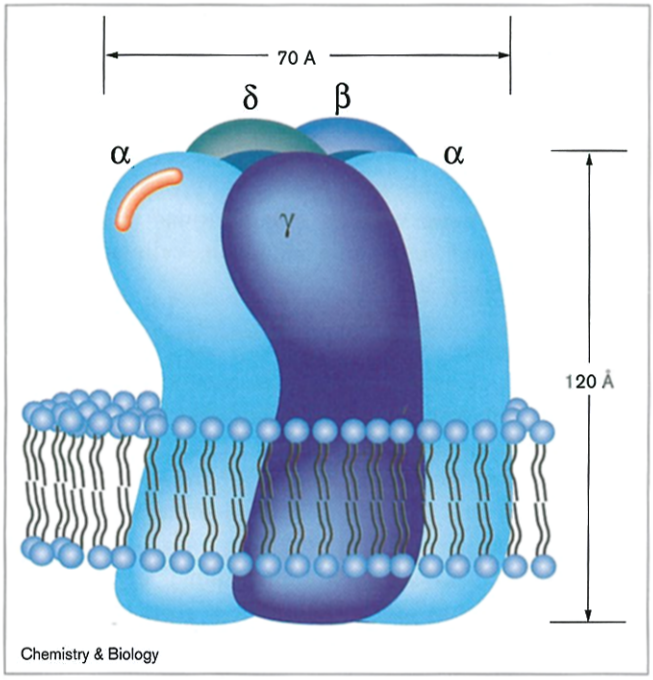

A schematic representation of the nAChR showing five homologous subunits in a roughly pentagonal array. Overall dimensions are taken from Unwin [38], but the arrangement of subunits is that advocated by a number of other workers [31,34,53]. The red bar on one of the α subunits denotes the approximate location of a main immunogenic region (MIR) [42].

the α70 biocytin mutant was expressed as a positive control so that whole-cell currents, which often vary substantially between oocyte batches, could be compared to an internal standard. A summary of these experiments is shown in Figure 5. Again, uncharged tRNA was tested at all the sites as a control. In all cases the current evoked from 200 μM ACh was less than 20% of that obtained in

Table 1

Sequence analysis of the MIR from 34 nAChR α subunits in the SWISS-PROT database.

Position	Conservation in α subunits (%)	ACh response with biocytin incorporation
Trp67*	97	–
Asn68	56	+
Pro69	79	–
Asp70	26	+
Asp71	53	+
Tyr72*	91	–
Gly73	47	–
Gly74*	82	–
Val75	62	+
Lys76	44	+

*Positions that have > 70% conservation across all nicotinic subunits (i.e. not solely α subunits). ACh, acetylcholine.

Figure 4

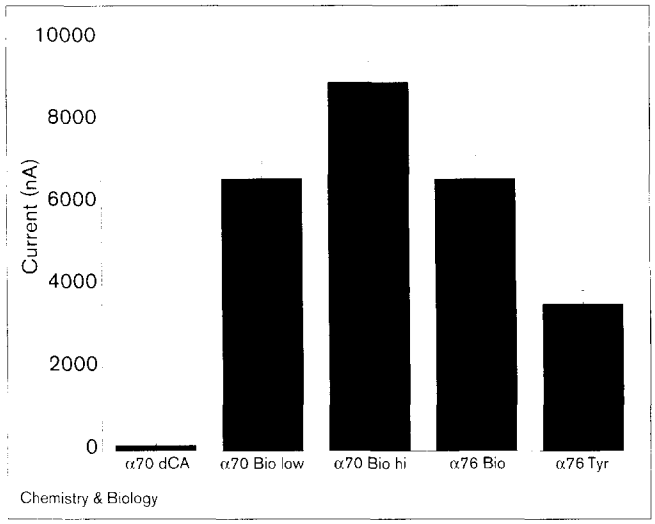

Average whole-cell currents in response to 200 μM acetylcholine (ACh) for oocytes injected with nAChR α70 TAG or α76 TAG – 4:1:1:1, 1.2 ng – and uncharged tRNA, or tRNA charged with biocytin (Bio) or tyrosine (Tyr). The two bars for the α70 biocytin are the averages of the currents for the five lowest expressing oocytes (low) and the five highest expressing oocytes (hi). Error bars are ± s.e.m. ($n = 5$).

Figure 5

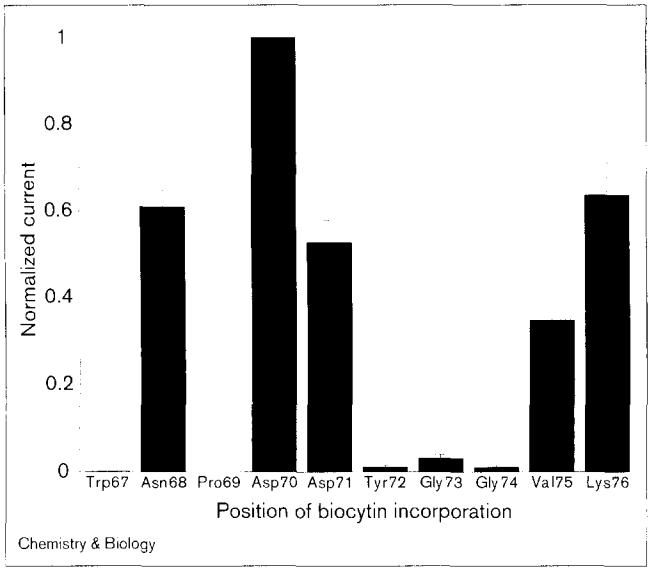

Whole-cell currents in response to 200 μM ACh from attempted biocytin suppression experiments at each of the ten positions of the MIR of the nAChR. Results are normalized to the whole-cell current of α70 biocytin expressed in the same experiment. Bars represent the mean of two experiments, each with five oocytes.

the suppression experiment, and in nine out of ten cases it was < 5% (data not shown).

The electrophysiology experiments clearly established the presence of functional, biocytin-containing ACh receptors on the oocyte surface for five of the ten positions in the MIR. Sequence conservation analysis of 34 nAChR α subunits shows that biocytin produced functional receptors at five of the six least conserved positions in the MIR (Table 1). The fact that biocytin did not express well at the sixth position (αGly73) may arise because a glycine (sidechain molecular weight = 1) to biocytin (sidechain molecular weight = 298) mutation may epitomize the phrase 'non-conservative mutation'. Furthermore, the four most highly conserved residues, three of which are conserved by > 70% across all nicotinic subunits, are the positions at which biocytin did not express. Because these four residues are highly conserved, they may be crucial for the structure or function of the receptor and even non-conservative conventional mutations may not be tolerated. We believe that the low currents observed for attempted biocytin incorporation at these positions indicate that the relatively large sidechain of biocytin is not tolerated at these positions.

With electrophysiological evidence for functional biotinylated receptors, we turned our attention to the binding of streptavidin in order to assay the surface exposure of particular sidechains. To assay for streptavidin binding, batches of five oocytes, the whole-cell currents of which had previously been determined, were incubated in a solution of 300 pM ^{125}I-streptavidin for 2 h and then washed extensively (see Materials and methods section). Individual oocytes were measured in a γ counter. Of the five mutants that showed large whole-cell currents, only one (α70 biocytin) showed streptavidin binding above background levels. In addition, no streptavidin binding was observed with any of the five mutants that did not give large whole-cell currents or with cells expressing non-biotinylated nAChRs. The results of a typical experiment are shown in Figure 6.

In the case of α70 biocytin, the mutant that showed streptavidin binding, we also evaluated the binding of ^{125}I-labeled α-bungarotoxin — a snake toxin that is highly specific for the nAChR. We found that the amounts of streptavidin and α-bungarotoxin bound to α70 biocytin were similar, suggesting that all nAChRs were completely labeled by both α-bungarotoxin and streptavidin (data not shown). This also provides concrete biochemical evidence to support the electrophysiological evidence that the *in vivo* suppression method produces full-length protein incorporating only the desired amino acid. If this were not the case (i.e. if some nAChR was produced with a natural amino acid incorporated at the suppression site as a result of read through of the stop codon or reacylation of the tRNA), we would have expected the amount of α-bungarotoxin binding to exceed the amount of streptavidin binding.

To explore whether the streptavidin-binding sites and α-bungarotoxin-binding sites overlap, we incubated oocytes

Figure 6

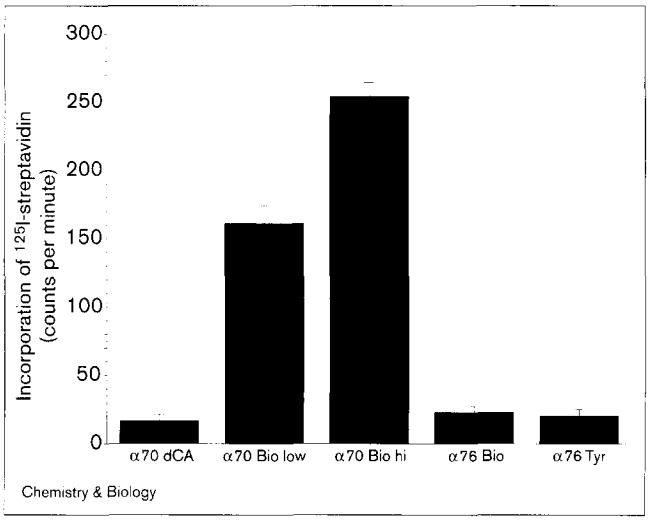

^{125}I-Streptavidin binding to oocytes injected with nAChR α70 TAG or α76 TAG and uncharged tRNA (dCA) or tRNA charged with biocytin (Bio) or tyrosine (Tyr). The oocytes used in this experiment are identical to those whose whole-cell currents are shown in Figure 4, demonstrating that binding of streptavidin correlates with whole-cell current. The α76Tyr mutation establishes that streptavidin does not bind to non-biotinylated nAChRs. Detector background has been subtracted in all cases. Error bars are ± s.e.m. ($n = 5$).

Figure 7

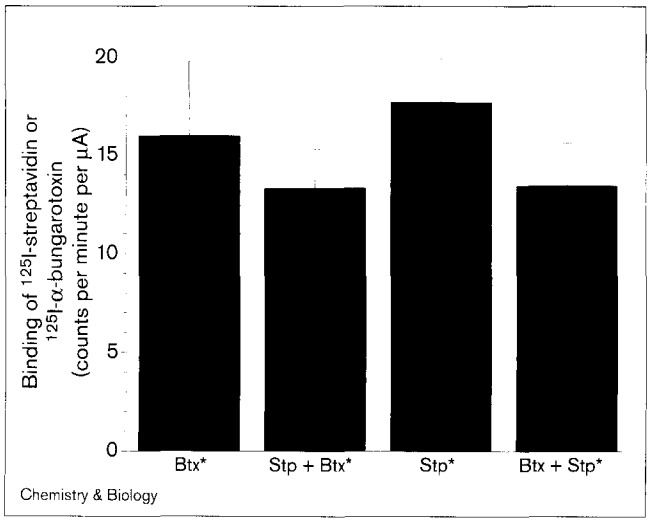

Whole-cell binding of ^{125}I-streptavidin and ^{125}I-α-bungarotoxin to AChR α70 biocytin mutants. Btx*, binding ^{125}I-α-bungarotoxin to untreated oocytes; Stp + Btx*, binding ^{125}I-α-bungarotoxin to oocytes pretreated with streptavidin; Stp*, binding ^{125}I-streptavidin to untreated oocytes; Btx + Stp*, binding ^{125}I-streptavidin to oocytes pretreated with α-bungarotoxin. Within the error bars shown, the data demonstrate that ^{125}I-α-bungarotoxin and ^{125}I-streptavidin do not interfere with one another in binding to the α70 biocytin nAChR. Binding is expressed as counts per minute per μA of whole-cell current, to account for different expression levels between groups of oocytes. Counts have been normalized to account for the differences in specific activity between the ^{125}I-streptavidin and ^{125}I-α-bungarotoxin. Error bars are ± s.e.m. ($n = 5$).

expressing nAChR α70 biocytin with unlabeled streptavidin. We then applied ^{125}I-α-bungarotoxin to these oocytes to determine if it could still bind. We also performed the reverse experiment, incubating oocytes expressing nAChR α70 biocytin with unlabeled α-bungarotoxin and attempting to bind ^{125}I-streptavidin. The results of these experiments are shown in Figure 7. These results clearly demonstrate that binding of α-bungarotoxin does not strongly inhibit binding of streptavidin to the α70 biocytin mutant and *vice versa*. This is consistent with previous studies, which demonstrated that both α-bungarotoxin and antibodies against the MIR are capable of binding simultaneously to the intact receptor [44].

Finally, we have measured the EC_{50} value (the dose at which 50% activation is seen) for ACh for the α70 biocytin mutant both before binding streptavidin (EC_{50} ~39 μM) and after binding (EC_{50} ~34 μM). These values are not significantly different from one another, nor are they significantly different from the EC_{50} value of the wild-type receptor (49 μM). At first it may seem surprising that the binding of a large protein to the receptor would not alter its pharmacological behavior, but previous studies have shown that antibodies binding to the MIR do not substantially alter the physiology of the receptor [45].

To gain a clearer physical picture of the above results, we have considered them in light of a previously published structural model. Tsikaris *et al.* [46] used nuclear magnetic resonance (NMR) spectroscopy to determine the structure of a ten residue peptide corresponding to the sequence of the MIR from the α subunit of the *Torpedo californica* nAChR. This sequence differs from that of the mouse muscle MIR studied here at two sites — Ala70 and Ile75. Starting with the coordinates for the *Torpedo* MIR taken from the Protein Data Bank [47,48], we altered the sidechain identities of these two residues to the corresponding mouse muscle residues (aspartate and valine, respectively) using standard geometries. The resulting structure is shown in Figure 8. The structure leads naturally to a rationalization of our results. The MIR peptide clearly has two sides — one that can tolerate biocytin and one that cannot. Biocytin is larger than any of the 20 natural amino acids, so perhaps it will produce functional receptors only if there is a pre-existing (or easily created) open space for its larger sidechain. We suggest that the 'blue' side has this open space, and so presumably faces away from the bulk of the protein. In contrast, the 'purple' side cannot tolerate biocytin and so apparently the sidechains on this face project down into the rest of the protein.

The selectivity of the biocytin method is shown by the result that biocytin was incorporated at five sites without loss of channel function and yet only one of these sites was competent to bind streptavidin under the conditions of

Figure 8

A schematic of the structure of the *Torpedo* MIR protein with modifications Ala70→Asp and Ile75→Val. Purple, sites at which biocytin incorporation was unsuccessful (α67, α69, α72, α73 and α74); blue, sites that incorporated biocytin, but did not bind streptavidin (α68, α71, α75 and α76); red, the sole streptavidin-binding site (α70). The right-hand view is derived from the left-hand view by a 180° rotation around a vertical axis.

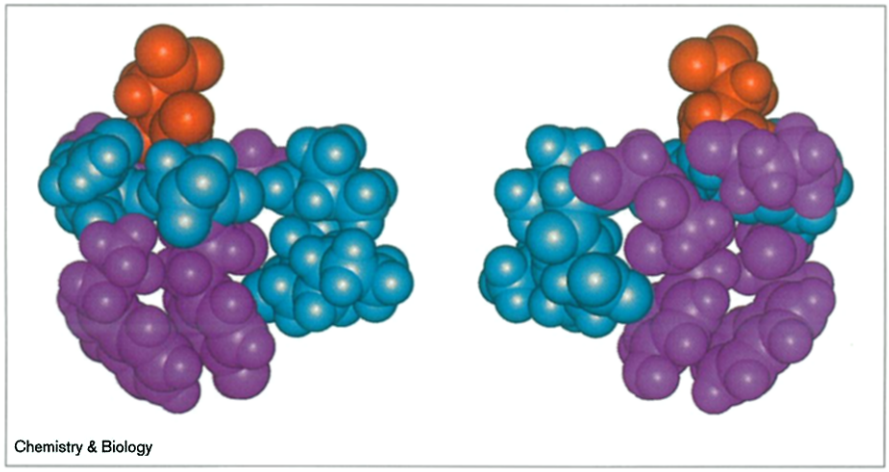

these experiments. The crystal structure of the biotin–streptavidin complex reveals that the ligand is buried fairly deeply in the protein, with even the terminal carboxylate not fully exposed [49]. Only residues that position the biocytin in an unencumbered environment will therefore lead to streptavidin binding. As shown in Figure 8, the Asp70 sidechain points 'up' and therefore away from, for example, the Trp67 or Tyr72 sidechains that are postulated to project down into the receptor. The other biotin-incorporating sidechains project approximately normal to the Asp70 sidechain. Apparently, these sites (α68, α71, α75, and α76) point to a space that is large enough for biocytin but not for streptavidin. There is precedent for binding interactions significantly weaker then 10^{-15} M^{-1} for substituted biotins [50], so perhaps higher streptavidin concentrations would have allowed detectable binding at the biotin-incorporating sites. Such studies were not feasible, however, due to non-specific binding of streptavidin to the oocytes at higher concentrations.

In summary, our results suggest a particular orientation for the MIR of the nAChR. Residue α70 points directly out and away from the receptor. The sidechains emanating from residues α67, α69, and α72 (α73 and α74 are glycines with effectively no sidechain) project down into the protein. The remaining residues, α68, α71, α75, and α76, project into open space, but perhaps towards some other structural feature of the receptor that prevents streptavidin binding. This analysis implies that a tether longer than is present in biocytin might allow streptavidin binding at the biotin-incorporating sites. We therefore prepared two longer chain analogs of biocytin, A and B (Figure 9). Unfortunately, we were not able to incorporate the longest analog, B, into functional receptors. We could incorporate biocytin-analog A at position α70 at levels that were readily detectable by electrophysiology (500–1000 nA). This is a remarkably 'unnatural' amino acid, suggesting considerable flexibility in the ribosomal machinery. The amount of expression achieved was not sufficient for the less sensitive streptavidin assay, however, and we were not, therefore, able to make use of the longer chain analog.

We conclude that the method of site-specific biocytin incorporation with streptavidin detection provides a potentially general way to identify highly surface-exposed residues in complex, integral membrane proteins. It thus provides information that goes beyond the 'simpler' question of transmembrane topology. We look forward to applying this approach to other channels, receptors, and transporters. Our data also show that biocytin derivatives with longer tethers do not express well, so the biocytin method alone cannot be simply generalized to a wide range of exposures. Alternative strategies can be envisioned, perhaps involving incorporation of unnatural residues which are rather small but which have specific reactivities allowing attachment of biotin moieties with longer chains.

Significance

Direct methods for determining the degree of exposure of individual residues in functional membrane proteins expressed in living cells would yield significant insight into membrane protein structure. Evaluation of the exposure also yields information about the transmembrane topology and more subtle variations in the intracellular and extracellular surface accessibility. The *in vivo* nonsense suppression method for the incorporation of unnatural amino acids into proteins is a powerful tool for obtaining atomic-scale information about functional proteins expressed in *Xenopus* oocytes. We have extended the method to allow incorporation of a biotinylated amino acid site-specifically within the main immunogenic region (MIR) of the nicotinic acetylcholine receptor (nAChR), the prototypical ligand-gated ion channel.

Figure 9

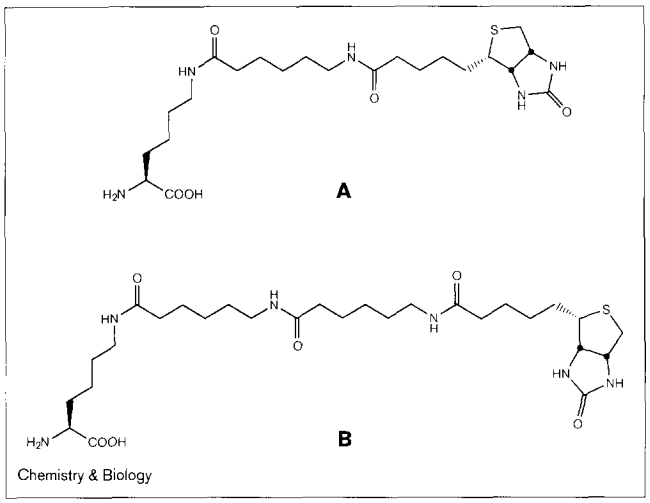

Two longer chain analogs of biocytin, A and B, that were used in an attempt to assess streptavidin binding.

Using ^{125}I-labeled streptavidin as a probe, we have been able to identify an amino acid in the MIR that is highly exposed on the surface of the nAChR. We believe that this method represents an improvement over previous approaches for determining surface exposure and transmembrane topology for a number of reasons: the method does not require purified protein; it uses a minimally perturbing point mutation; it uses a marker that is not endogenous to either the protein of interest or to other cell-surface proteins; it allows detection by a commercially available assay; and it determines the topology and surface exposure in a functional, characterizable protein expressed *in vivo*. Thus, we consider the method to be a potentially general one for determining the surface exposure of specific residues of transmembrane proteins expressed *in vivo*. In a broader sense, these results demonstrate the power of the *in vivo* nonsense suppression method for applying the tools of organic chemistry to the problems of molecular neuroscience.

Materials and methods

Reagents were purchased from Aldrich unless otherwise noted. (3-[^{125}I]-iodotyrosyl^{54})α-bungarotoxin (2000 mCi/mmol) and [^{125}I]-streptavidin (30 mCi/mg) were purchased from Amersham. Anhydrous THF was distilled from Na/benzophenone; anhydrous DMF was obtained from Aldrich. All chemical syntheses were performed under a positive pressure of argon unless noted otherwise. NMR spectra were recorded on a General Electric QE300 (300 MHz ^{1}H, 75 MHz ^{13}C), JEOL Delta 400 (100 MHz, ^{13}C), or a Bruker AM-500 (500 MHz ^{1}H, 125 MHz ^{13}C) spectrometer and are referenced to residual solvent protons. Mass spectrometry (FAB) was performed by the mass spectrometry facilities at the University of California, Riverside, USA or at Caltech, CA, USA. Ultra-violet/visible (UV/vis) spectra were recorded on a Beckman Instruments DU-640 continuous-wave spectrometer. High performance liquid chromatography (HPLC) separations were performed on a Waters dual 510 pump liquid chromatograph system equipped with either a Waters 490E variable wavelength UV detector or a Waters 960 photo diode array detector. Analytical HPLC samples were separated using a Waters NovaPak C18 column (3.9 × 150 mm); semi-preparative samples were separated using a Whatman Magnum 9 column (9.4 × 500 mm, Partisil 10, ODS-3). Oligonucleotides for mutagenesis were synthesized by the Biopolymer Synthesis Facility at Caltech. Polymerase chain reactions (PCR) were performed using a Perkin-Elmer TC-1 DNA Thermal Cycler. Automated sequencing of PCR products was performed by the DNA Sequencing Core Facility at Caltech. Ligation of aminoacyl-dCA to tRNA-THG73(-CA) was performed as described previously [29].

NVOC-biocytin cyanomethyl ester

Biocytin (50 mg, 0.13 mmol, Molecular Probes) and sodium carbonate (28 mg, 0.27 mmol) were dissolved with stirring in water (7.5 ml) and freshly distilled THF (5 ml). A solution of 6-nitroveratryloxycarbonyl chloride (NVOC-Cl) (37 mg, 0.13 mmol) in 5 ml THF was added dropwise [30,51]. After 3 h, solvents were removed *in vacuo* and the remaining residue was dissolved in dry DMF (1.5 ml) and chloroacetonitrile (1.5 ml). Triethylamine (400 µl) was added and the mixture was stirred overnight. Volatiles were removed *in vacuo* and the remaining solid was purified by flash chromatography (silica gel, CH_2Cl_2 + MeOH 1–10%) to give 67 mg of NVOC-biocytin cyanomethyl ester as a pale yellow solid (77% yield for 2 steps): ^{1}H NMR (500 MHz, DMSO-d_6) δ 8.10 (d-br, J = 6.8 Hz, 1H), 7.74 (t-br, J = 5.0 Hz, 1H), 7.70 (s, 1H), 7.18 (s, 1H), 6.39 (s, 1H), 6.33 (s, 1H), 5.38 (*AB*, J = 15.0 Hz, 1H), 5.34 (*AB*, J = 15.0 Hz, 1H), 5.01 (s, 2H), 4.27 (m, 1H), 4.11 (m, 1H), 3.92 (s, 3H), 3.86 (s, 3H), 3.13 (m, 1H), 3.04 (m, 1H), 2.99 (m, 2H), 2.80 (dd, J = 10 Hz, 5.5 Hz, 1H), 2.57-2.46 (m, 3H), 2.03 (t, 2H), 1.70-1.15 (m, 10H); ^{13}C NMR (75 MHz, DMSO-d_6) δ 172.0, 171.6, 162.8, 155.8, 153.5, 147.8, 139.2, 127.8, 115.8, 110.3, 108.2, 62.8, 61.1, 59.3, 56.3, 56.1, 55.5, 53.6, 49.5, 39.9, 38.1, 35.3, 30.2, 28.7, 28.3, 28.1, 25.4, 22.8.

α-NVOC-ε-(6-(biotinoyl)amino)hexanoyl-L-lysine (NVOC-A)

A solution of α-NVOC-lysine (42 mg, 0.11 mmol, 1.0 equivalent, prepared in two steps from ε-Boc-lysine and NVOC-Cl, followed by removal of the Boc-group with TFA), 6-((biotinoyl)amino)caproic acid N-hydroxysuccinimide ester (50 mg, 0.11 mmol, 1.0 equivalent, Molecular Probes) and Na_2CO_3 (47 mg, 0.44 mmol, 4.0 equivalent) was stirred in dry DMF (5 ml) under argon. After 3 days, the mixture had become gel-like and a solution of 1N $NaHSO_4$ (50 ml) was added, followed by CH_2Cl_2 (50 ml). The mixture was stirred and a pale yellow precipitate formed. The solid was filtered, washed with CH_2Cl_2, water, acetone, and dried to give 42 mg of a pale yellow solid (53% yield): ^{1}H NMR (500 MHz, DMSO-d_6) δ 7.74 (d-br, J = 8 Hz, 1H), 7.66 (m, 2H), 7.64 (s, 1H), 7.12 (s, 1H), 6.39 (s, 1H), 6.33 (s, 1H), 5.33 (*AB*, J = 15.1Hz, 1H), 5.25 (*AB*, J = 15.1 Hz, 1H), 4.23 (t, J = 5.5 Hz, 1H), 4.06 (m, 1H), 3.85 (s, 3H), 3.80 (s, 3H), 3.02 (m, 1H), 2.93 (m, 4 H), 2.82 (s, 1H), 2.76 (m, 1H), 2.73 (s, 1H), 2.50 (d, J = 12.4 Hz, 1H), 1.94 (m, 4H), 1.63 (m, 1H), 1.52 (m, 2H), 1.37 (m, 4H), 1.28 (m, 8H), 1.15 (m, 2H); ^{13}C NMR (100 MHz, DMSO-d_6) δ 173.8, 171.9, 171.8, 162.7, 155.8, 153.5, 147.6, 139.0, 138.1, 128.2, 110.0, 108.1, 62.4, 61.0, 59.2, 56.2, 56.1, 55.4, 53.8, 38.3, 38.1, 35.4, 35.2, 30.4, 28.9, 28.7, 28.2, 28.0, 26.1, 25.3, 25.0, 23.0.

α-NVOC-ε-(6-(biotinoyl)amino)hexanoyl-L-lysine cyanomethyl ester

To a solution of α-NVOC-ε-(6-(biotinoyl)amino)hexanoyl-L-lysine (40 mg, 0.055 mmol, 1.0 equivalent) in 2 ml dry DMF was added triethylamine (24 µl, 0.165 mmol, 3.0 equivalents) and chloroacetonitrile (2 ml). After stirring for 9 h under argon, volatiles were removed *in vacuo* and the remaining solid was partitioned between water and CH_2Cl_2. A pale yellow solid remained and was combined with the organic fraction, concentrated and dried *in vacuo* to afford the cyanomethyl ester as a pale yellow solid (20 mg, 47%): ^{1}H NMR (500 MHz, DMSO-d_6) δ 8.07 (d, J = 7.5 Hz, 1H), 7.70 (m, 2H), 7.18 (s, 1H), 6.39 (s, 1H), 6.33 (s, 1H), 5.38 (*AB*, J = 14.8 Hz, 1H), 5.34 (*AB*, J = 14.8 Hz, 1H), 5.01 (s, 2H), 4.29 (t, J = 5.6 Hz, 1H), 4.12 (m, 2H), 3.92 (s, 3H), 3.86 (s, 3H), 3.08 (m, 1H), 2.97 (m, 4H), 2.80 (s, 1H), 2.57-2.49 (m, 2H), 2.01 (m, 4H), 1.63 (m, 1H), 1.43 (m, 4H), 1.34 (m, 8H), 1.17 (m, 2H).

α-NVOC-ε-(6-((6-((biotinoyl)amino)hexanoyl)amino)hexanoyl)-L-lysine (NVOC-B) fluorenylmethyl ester

A mixture of 6-((6-((biotinoyl)amino)hexanoyl)amino)hexanoic acid, succinimidyl ester (50 mg, 0.088 mmol, 1 equivalent) and α-NVOC-lysine fluorenylmethyl ester (75 mg, 0.13 mmol, 1.5 equivalents; [52]) was stirred in dry DMF (1 ml) with triethylamine (25 µl, 2 equivalents). The reaction was stirred for 4 days after which time the volatiles were removed and the yellow residue was purified by column chromatography (silica, 4:1 CH_2Cl_2:MeOH) to afford 46 mg of the desired product (47% yield): ^{1}H NMR (500 MHz, DMSO-d_6) δ 7.92-7.84 (m, 3H), 7.69-7.55 (m, 6 H), 7.36 (q, J = 7.6 Hz, 2H), 7.25 (m, 2H), 7.13 (s, 1H), 6.35 (s, 1H), 6.30 (s, 1H), 5.34 (*AB*, J = 13.5 Hz, 1H), 5.28 (*AB*, J = 13.5 Hz, 1H), 4.45 (m, 1H), 4.38 (m, 1H), 4.23 (m, 1H), 4.19 (t, J = 5.0 Hz, 1H), 4.07 (m, 1H), 3.89 (q, J = 7.0 Hz, 1H), 3.84 (s, 3H), 3.80 (s, 3H), 3.05 (m, 1H), 2.75 (m, 1H), 1.97 (m, 6H), 1.65-1.20 (m, 26H); ^{13}C NMR (125 MHz, DMSO-d_6) δ 172.0, 171.6, 171.5, 162.4, 155.5, 153.2, 147.5, 144.0, 143.4, 140.5, 139.0, 127.5, 127.4, 126.8, 124.7, 119.8, 110.3, 108.0, 65.5, 62.2, 60.8, 59.0, 55.9, 55.9, 55.1, 53.7, 46.1, 40.3, 38.0, 37.8, 35.1, 35.0, 29.9, 28.7, 28.4, 27.9, 27.7, 25.9, 25.0, 24.8, 22.5.

α-NVOC-ε-(6-((6-((biotinoyl)amino)hexanoyl)amino)hexanoyl)-L-lysine cyanomethyl ester

α-NVOC-ε-(6-((6-((biotinoyl)amino)hexanoyl)amino)hexanoyl)-L-lysine fluorenylmethyl ester (19 mg, 0.02 mmol, 1 equivalent) was dissolved in dry DMF (1 ml). Piperidine (20 µl, 10 equivalents) was added and the mixture was stirred. After 2.5 h, volatiles were removed *in vacuo*, hexane (15 ml) was added, and the suspension was filtered. The remaining solid was dissolved in aqueous DMF. The solution was lyophilized and the solid residue was dissolved in dry DMF (4 ml), chloroacetonitrile (0.8 ml) and triethylamine (100 µl). After 24 h, the mixture was separated using preparative HPLC with a linear gradient of 100% 10 mM aqueous acetic acid to 100% acetonitrile over 1 h. The product-containing fractions were lyophilized to give 5 mg of a pale yellow solid (31% yield for 2 steps): ^{1}H NMR (500 MHz, DMSO-d_6) δ 8.08 (d, J=7.5 Hz, 1H), 7.95 (s, 1H), 7.18 (s, 1H), 6.40 (s, 1H), 6.34 (s, 1H), 5.40 (*AB*, J = 14.8 Hz, 1H), 5.35 (*AB*, J = 14.8 Hz, 1H), 5.01 (s, 2H), 4.31 (m, 1H), 4.12 (m, 2H), 3.92 (s, 3H), 3.86 (s, 3H), 3.07 (m, 1H), 2.98 (m, 6 H), 2.88 (s, 1H), 2.80 (dd, J=7.3, 5.2 Hz, 1H), 2.72 (s, 1H), 2.57 (d, J=12.4 Hz, 1H), 1.75-1.52 (m, 4H), 1.50-1.41 (m, 6H), 1.41-1.25 (m, 8H), 1.25-1.12 (m, 4H); ^{13}C NMR (125 MHz, DMSO-d_6) δ 171.8, 171.7, 171.3, 162.5, 162.2, 155.6, 153.4, 148.6, 139.3, 127.5, 115.5, 110.5, 108.3, 66.9, 62.5, 61.0, 59.1, 56.1, 56.1, 55.2, 53.5, 49.7, 49.3, 44.2, 38.2, 37.9, 35.6, 35.3, 35.1, 30.7, 28.8, 28.5, 28.0, 27.9, 26.0, 25.2, 24.9, 24.8, 22.6.

General method for coupling of N-protected amino acids to dCA

This method is essentially as described [26,30]. The N-protected amino acid (~30 µmol, 3 equivalents) was mixed with the tetra-*n*-butylammonium salt of the dCA dinucleotide (~10 µmol, 1 equivalent) in dry DMF (400 µl). The reactions were monitored by analytical HPLC with a linear gradient of 100% 25 mM aqueous ammonium acetate buffer (pH 4.5) to 100% acetonitrile over 1 h. Following the disappearance of the dCA (5 min to 3 h), the reaction mixture was separated using semi-preparative HPLC with a linear gradient of 100% 25 mM aqueous ammonium acetate buffer (pH 4.5) to 100% acetonitrile. The fractions containing the aminoacyl dinucleotide were collected and lyophilized. The lyophilized solid was redissolved in 10 mM aqueous acetic acid/acetonitrile and lyophilized a second time to remove salts. The products were characterized by UV/vis and mass spectrometry.

dCA-NVOC-biocytin

Prepared as above: FAB-MS [M–H]$^-$ 1228, calc'd for $C_{45}H_{61}N_{13}O_{22}P_2S$ 1228; UV λ_{max} (10 mM aqueous acetic acid) 258 nm, 350 nm.

dCA-α-NVOC-ε-(6-(biotinoyl)amino)hexanoyl-L-lysine

Prepared as above: FAB-MS [M–H]$^-$ 1342, calc'd for $C_{51}H_{72}N_{14}O_{23}P_2S$ 1342; UV λ_{max} (10 mM aqueous acetic acid) 256 nm, 350 nm.

dCA-α-NVOC-ε-(6-((6-((biotinoyl)amino)hexanoyl)amino)-hexanoyl)-L-lysine

Prepared as above: ESI-MS [M+Na]$^+$ 1480, calc'd for $C_{57}H_{80}N_{15}O_{24}P_2SNa$ 1480; UV λ_{max} (10 mM aqueous acetic acid) 253 nm, 350 nm.

Site-directed mutagenesis of the AChR α67-76 TAG mutants

The mouse muscle AChR α67–76 TAG mutants were prepared using a standard two step PCR-based cassette mutagenesis procedure using *Pfu* Polymerase (Stratagene). For each mutant, a trimmed *BsmBI-MscI* PCR-generated fragment was subcloned into the dephosphorylated *BsmBI-MscI* fragment of mouse muscle AChR α subunit in the pAMV-PA vector [28]. When possible, silent mutations were introduced to facilitate screening of positive colonies by restriction endonuclease digestion. We have found the *BfaI* recognition sequence CTAG to be particularly helpful for screening. All mutants were verified by automated sequencing of the entire PCR cassette across both ligation sites.

In vitro *transcription of mRNA*

mRNA was synthesized *in vitro* from *NotI* linearized plasmid DNA (1 µg/20 µl reaction) using the T7 MessageMachine kit from Ambion as described in the manufacturer's instructions. The products were purified by phenol:chloroform:isoamyl alcohol extraction and isopropanol precipitation. Purity of the mRNA was assayed by gel electrophoresis.

Oocyte preparation and injection

Oocytes were removed from *Xenopus laevis* as described previously [43] and maintained at 18°C in ND96 solution consisting of 96 mM NaCl, 2 mM KCl, 1 mM $MgCl_2$, 1.8 mM $CaCl_2$, 5 mM HEPES (pH 7.5), supplemented with sodium pyruvate (2.5 mM), gentamicin (50 µg/ml), theophylline (0.6 mM) and horse serum (5%). Prior to microinjection, the NVOC-aminoacyl-tRNA (1 µg/µl in 1 mM NaOAc, pH 5.0) was deprotected by irradiating the sample for 5 min with a 1000 W xenon arc lamp (Oriel) operating at 600 W equipped with WG-335 and UG-11 filters (Schott). The deprotected aminoacyl-tRNA was mixed 1:1 with a water solution of the desired mRNA. Oocytes were injected with 50 nl of a mixture containing 25 ng aminoacyl-tRNA and 1.2 ng of total mRNA (4:1:1:1 α:β:γ:δ subunit stoichiometry).

Electrophysiology

Two-electrode voltage clamp measurements were performed 36–48 h after injection using a GeneClamp 500 amplifier (Axon Instruments, Foster City, CA, USA). Microelectrodes were filled with 3 M KCl and had resistances of 0.5–2 MΩ. Oocytes were perfused with a nominally calcium-free bath solution containing 96 mM NaCl, 2 mM KCl, 1 mM $MgCl_2$, 5 mM HEPES (pH 7.5). Macroscopic ACh-induced currents were recorded in response to application of 200 µM ACh at a holding potential of −80 mV. Whole cell current measurements are reported as the mean ± standard error.

General procedure for radioactive ligand-binding experiments

Batches of five oocytes were incubated at room temperature for 15 min with gentle agitation in 400 µl calcium-free ND96 (see Electrophysiology section) containing 10 mg/ml BSA (FractionV, Sigma). The radioactive ligand was then added to a final concentration of 300 pM for ^{125}I-streptavidin (Amersham, 30 µCi/µg) or 1 nM for ^{125}I-α-bungarotoxin (Amersham, 2000 Ci/mmol). After 2 h, the oocytes were transferred to an ice-cold solution of ND96 + 10 mg/ml BSA (1.5 ml) and agitated for 5 min. The oocytes were then washed extensively in fresh solutions of ice-cold ND96 + BSA and transferred individually to scintillation vials and counted in a Beckman LS5000 γ-counter. In all cases, a sample of the final wash solution was counted to ensure that unbound ligand had not been carried through the assay. In addition, five empty scintillation vials were counted in each experiment to determine the detector background which was then subtracted from subsequent measurements. In experiments involving the binding of both labeled and unlabeled ligand, the unlabeled ligand was added at high concentration (166 nM for streptavidin, 312 nM for bungarotoxin) to the initial 400 µl solution. After 20 min, the labeled ligand was added and the assay proceeded as described above.

Acknowledgements

This work was supported by the National Institutes of Health (NS-34407 and NS-11756). J.P.G. is grateful to Caltech and to the Eastman Kodak Corporation for support in the form of graduate fellowships. We thank Scott K. Silverman for providing a sample of α-NVOC-lysine fluorenylmethyl ester.

References

1. White, S.H., ed. (1994). *Membrane Protein Structure. Methods in Physiology*. Oxford University Press Inc., New York.
2. Hollmann, M., O'Shea-Greenfield, A., Rogers, S.W. & Heinemann, S. (1989). Cloning by functional expression of a member of the glutamate receptor family. *Nature* **342**, 643-648.
3. Hollmann, M., Maron, C. & Heinemann, S. (1994). N-glycosylation site tagging suggests a three transmembrane domain topology for the glutamate receptor GluR1. *Neuron* **13**, 1331-1343.
4. Bennett, J.A. & Dingledine, R. (1995). Topology profile for a glutamate receptor: three transmembrane domains and a channel-lining reentrant membrane loop. *Neuron* **14**, 373-384.
5. Schwalbe, R.A., Wang, Z., Bianchi, L. & Brown, A.M. (1996). Novel sites of *N*-glycosylation in ROMK1 reveal the putative pore-forming segment H5 as extracellular. *J. Biol. Chem.* **271**, 24201-24206.
6. Bennett, E.R. & Kanner, B.I. (1997). The membrane topology of GAT-1, a (Na^+ + Cl^-)-coupled γ-aminobutyric acid transporter from rat brain. *J. Biol. Chem.* **272**, 1203-1210.
7. Olivares, L., Aragón, C., Giménez, C. & Zafra, F. (1997). Analysis of the transmembrane topology of the glycine transporter GLYT1. *J. Biol. Chem.* **272**, 1211-1217.
8. Turk, E., Kerner, C.J., Lostao, M.P. & Wright, E.M. (1996). Membrane topology of the human Na^+/glucose co-transporter SGLT1. *J. Biol. Chem.* **271**, 1925-1934.
9. Pedemonte, C.H., Sachs, G. & Kaplan, J.H. (1990). An intrinsic membrane glycoprotein with cytosolically oriented N-linked sugars. *Proc. Natl Acad. Sci. USA* **87**, 9789-9793.
10. Chang, X.B., Hou, Y.X., Jensen, T.J. & Riordan, J.R. (1994). Mapping of cystic fibrosis transmembrane conductance regulator membrane topology by glycosylation site insertion. *J. Biol. Chem.* **269**, 18572-18575.
11. Frillingos, S. & Kaback, H.R. (1996). Probing the conformation of the lactose permease of *Escherichia coli* by *in situ* site-directed sulfhydryl modification. *Biochemistry* **35**, 3950-3956.
12. Loo, T.W. & Clarke, D.M. (1995). Membrane topology of a cysteine-less mutant of human P-glycoprotein. *J. Biol. Chem.* **270**, 843-848.
13. Sun, J., Li, J., Carrasco, N. & Kaback, H.R. (1997). The last two cytoplasmic loops in the lactose permease of *Escherichia coli* comprise a discontinuous epitope for a monoclonal antibody. *Biochemistry* **36**, 274-280.
14. Slatin, S.L., Qiu, X.Q., Jakes, K.S. & Finkelstein, A. (1994). Identification of a translocated protein segment in a voltage-dependent channel. *Nature* **371**, 158-161.
15. Akabas, M.H., Stauffer, D.A., Xu, M. & Karlin, A. (1992). Acetylcholine receptor channel structure probed in cysteine-substitution mutants. *Science* **258**, 307-310.
16. Javitch, J.A., Fu, D., Chen, J. & Karlin, A. (1995). Mapping the binding-site crevice of the dopamine D2 receptor by the substituted-cysteine accessibility method. *Neuron* **14**, 825-831.
17. Chavez, R.A. & Hall, Z.W. (1992). Expression of fusion proteins of the nicotinic acetylcholine receptor from mammalian muscle identifies the membrane-spanning regions in the α and δ subunits. *J. Cell Biol.* **116**, 385-393.
18. Anand, R., Bason, L., Saedi, M.S., Gerzanich, V., Peng, X. & Lindstrom, J. (1993). Reporter epitopes: a novel approach to examine transmembrane topology of integral membrane proteins applied to the α1 subunit of the nicotinic acetylcholine receptor. *Biochemistry* **32**, 9975-9984.
19. Mund, M., Weise, C., Franke, P. & Hucho, F. (1997). Mapping of exposed surfaces of the nicotinic acetylcholine receptor by identification of iodinated tyrosine residues. *J. Protein Chem.* **16**, 161-170.
20. Green, N.M. (1975). Avidin. *Adv. Protein Chem.* **29**, 85-133.
21. Wilchek, M. & Bayer, E.A., eds (1990). *Avidin-Biotin Technology. Methods in Enzymology*. Academic Press Inc., San Diego, CA, USA.
22. Hofmann, K., Titus, G., Montibeller, J.A. & Finn, F.M. (1982). Avidin binding of carboxyl-substituted biotin and analogues. *Biochemistry* **21**, 978-984.
23. Kurzchalia, T., Wiedmann, M., Breter, H., Zimmermann, W., Bauschke, E. & Rapoport, T.A. (1988). tRNA-mediated labelling of proteins with biotin. A nonradioactive method for the detection of cell-free translation products. *Eur. J. Biochem.* **172**, 663-668.
24. Noren, C.J., Anthony-Cahill, S.J., Griffith, M.C. & Schultz, P.G. (1989). A general method for site-specific incorporation of unnatural amino acids into proteins. *Science* **244**, 182-188.
25. Ellman, J., Mendel, D., Anthonycahill, S., Noren, C.J. & Schultz, P.G. (1991). Biosynthetic method for introducing unnatural amino-acids site-specifically into proteins. *Methods Enzymol.* **202**, 301-336.
26. Robertson, S.A., Ellman, J.A. & Schultz, P.G. (1991). A general and efficient route for chemical aminoacylation of transfer RNAs. *J. Am. Chem. Soc.* **113**, 2722-2729.
27. Cornish, V.W., Mendel, D. & Schultz, P.G. (1995). Probing protein structure and function with an expanded genetic code. *Angew. Chem. Int. Ed. Engl.* **34**, 621-633.
28. Nowak, M.W., *et al.*, & Lester, H.A. (1995). Nicotinic receptor binding site probed with unnatural amino-acid incorporation in intact cells. *Science* **268**, 439-442.
29. Saks, M.E., *et al.*, & Dougherty, D.A. (1996). An engineered *tetrahymena* $tRNA^{Gln}$ for *in vivo* incorporation of unnatural amino acids into proteins by nonsense suppression. *J. Biol. Chem.* **271**, 23169-23175.
30. Kearney, P.C., Nowak, N.W., Zhong, W., Silverman, S.K., Lester, H.A. & Dougherty, D.A. (1996). Dose-response relations for unnatural amino acids at the agonist binding site of the nicotinic acetylcholine receptor: tests with novel side chains and with several agonists. *Mol. Pharmacol.* **50**, 1401-1412.
31. Kearney, P.C., Zhang, H., Zhong, W., Dougherty, D.A. & Lester, H.A. (1996). Determinants of nicotinic receptor gating in natural and unnatural side chain structures at the M2 9′ position. *Neuron* **17**, 1221-1229.
32. England, P.M., Lester, H.A., Davidson, N. & Dougherty, D.A. (1997). Site-specific, photochemical proteolysis applied to ion channels *in vivo*. *Proc. Natl Acad. Sci. USA*, in press.
33. Turcatti, G., *et al.*, & Chollet, A. (1996). Probing the structure and function of the tachykinin neurokinin-2 receptor through biosynthetic incorporation of fluorescent amino acids at specific sites. *J. Biol. Chem.* **271**, 19991-19998.
34. Karlin, A. (1993). Structure of nicotinic acetylcholine receptors. *Curr. Opin. Neurobiol.* **3**, 299-309.
35. Devillers-Thiéry, A., Galzi, J.L., Eisel, J.L., Bertrand, S., Bertrand, D. & Changeux, J.P. (1993). Functional architecture of the nicotinic acetylcholine receptor: a prototype of ligand-gated ion channels. *J. Membrane Biol.* **136**, 97-112.
36. Lester, H.A. (1992). The permeation pathway of neurotransmitter-gated ion channels. *Annu. Rev. Biophys. Biomol. Struct.* **21**, 267-292.
37. Stroud, R.M., McCarthy, M.P. & Shuster, M. (1990). Nicotinic acetylcholine receptor superfamily of ligand-gated ion channels. *Biochemistry* **29**, 11009-11023.
38. Unwin, N. (1993). Nicotinic acetylcholine receptor at 9 Å resolution. *J. Mol. Biol.* **229**, 1101-1124.
39. Kubalek, E., Ralston, S., Lindstrom, J. & Unwin, N. (1987). Location of subunits within the acetylcholine receptor by electron image analysis of tubular crystals from *Torpedo marmorata*. *J. Cell Biol.* **105**, 9-18.
40. Tzartos, S.J., *et al.*, & Tsikaris, V. (1991). The main immunogenic region (MIR) of the nicotinic acetylcholine receptor and the anti-MIR antibodies. *Mol. Neurobiol.* **5**, 1-29.
41. Mamalaki, A. & Tzartos, S.J. (1994). Nicotinic acetylcholine receptor: structure, function and main immunogenic region. *Adv. Neuroimmunol.* **4**, 339-354.
42. Beroukhim, R. & Unwin, N. (1995). Three-dimensional location of the main immunogenic region of the acetylcholine receptor. *Neuron* **15**, 323-331.
43. Quick, M. & Lester, H.A. (1994). Methods for expression of excitability proteins in *Xenopus* Oocytes. In *Ion Channels of Excitable Cells*. (Narahashi, T., ed.), pp 261-279, Academic Press, San Diego, CA, USA.
44. Verrall, S. & Hall, Z.W. (1992). The N-terminal domains of acetylcholine receptor subunits contain recognition signals for the initial steps of receptor assembly. *Cell* **68**, 23-31.
45. Tamamizu, S., Butler, D.H., Lasalde, J.A. & McNamee, M.G. (1996). Effects of antibody binding on structural transitions of the nicotinic acetylcholine receptor. *Biochemistry* **35**, 11773-11781.

46. Tsikaris, V., *et al.*, & Cung, M.T. (1993). Conformational requirements for molecular recognition of acetylcholine receptor main immunogenic region (MIR) analogues by monoclonal anti-MIR antibody: a two-dimensional nuclear magnetic resonance and molecular dynamics approach. *Biopolymers* **33**, 1123-1134.
47. Abola, E.E., Bernstein, F.C., Bryant, S.H., Koetzle, T.F. & Weng, J. (1987). Protein data bank. In *Crystallographic Databases-Information Content, Software Systems, Scientific Applications.* (Allen, F.H., Bergerhoff, G. & Sievers, R., eds), pp 107-132, Data Commission of the International Union of Crystallography, Bonn/Cambridge/Chester, UK.
48. Bernstein, F.C., *et al.*, & Tasumi, M. (1977). The Protein Data Bank: a computer-based archival file for macromolecular structures. *J. Mol. Biol.* **112**, 535-542.
49. Weber, P.C., Ohlendorf, D.H., Wendoloski, J.J. & Salemme, F.R. (1989). Structural origins of high-affinity biotin binding to streptavidin. *Science* **243**, 85-88.
50. Fujita, K. & Silver, J. (1993). Surprising lability of biotin-streptavidin bond during transcription of biotinylated DNA bound to paramagnetic streptavidin beads. *Biotechniques* **14**, 608-617.
51. Amit, B., Zehavi, U. & Patchornik, A. (1974). Photosensitive protecting groups of amino sugars and their use in glycoside synthesis. 2-Nitrobenzyloxycarbonylamino and 6-nitroveratryloxycarbonylamino derivatives. *J. Org. Chem.* **39**, 192-196.
52. Silverman, S.K. (1998). I. Conformational and Charge Effects on High-Spin Polyradicals. II. Studies on the Chemical-Scale Origin of Ion Selectivity in Potassium Channels, *Ph.D. Thesis.* California Institute of Technology, CA, USA.
53. Machold, J., Weise, C., Utkin, Y., Tsetlin, V. & Hucho, F. (1995). The handedness of the subunit arrangement of the nicotinic acetylcholine receptor from *Torpedo californica*. *Eur. J. Biochem.* **234**, 427-430.